International Journal of Computer Science in Sport

Volume 18, Issue 2 (Special Edition), 2019

Journal homepage: http://iacss.org/index.php?id=30

sciendo

DOI: 10.2478/ijcss-2019-0014

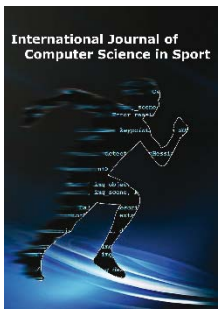

Energy Cost Of Running Under Hypogravity In Well-Trained Runners And Triathletes: A Biomechanical Perspective

Ueberschär, O.[1,2], Fleckenstein, D.[1,3], Warschun, F.[1], Walter, N.[1], Wüstenfeld, J. C.[1,4], Wolfarth, B.[1,4], Hoppe, M. W.[5,6]

[1] *Institute for Applied Training Science (IAT); Leipzig, Germany*

[2] *Magdeburg-Stendal University of Applied Sciences; Magdeburg, Germany*

[3] *German Athletics Association; Dortmund, Leipzig, Darmstadt, Germany*

[4] *Department of Sports Medicine, Humboldt University / Charité – Universitätsmedizin, Berlin*

[5] *Department of Movement and Training Science, University of Wuppertal; Wuppertal, Germany*

[6] *Department of Orthopaedics, Trauma and Hand Surgery, Klinikum Osnabrück GmbH; Osnabrück, Germany*

Abstract

Hypogravity treadmills have become a popular training tool in distance running and triathlon. Counter-intuitively, tibial acceleration load is not attenuated by hypogravity unloading during running, while, equally surprisingly, leaps become flatter instead of higher. To explain these effects from a biomechanical perspective, Polet, Schroeder, and Bertram (2017) recently developed an energetic model for hypogravity running and validated it with recreational athletes at a constant jogging speed. The present study was conducted to refine that model for competitive athletes at relevant running speeds of 12–22 km h^{-1} and gravity levels of 100 %, 80 % and 60 %. Based on new experimental data on 15 well-trained runners in treadmill tests until volitional exhaustion, the enhanced semi-empirical model well describes energy expenditure and the observed biomechanical effects of hypogravity running. Remarkably, anaerobic contributions led to an increase in energy cost per meter for speeds above 16–18 km h^{-1} ($p < 0.001$), irrespective of hypogravity unloading. Moreover, some converging trends were observed that might reflect general adaptations in running motor control for optimization of efficiency. In essence, the outcome of this research might help sports scientists and practitioners to design running programs for specific training stimuli, e.g. conditioning of anaerobic energy metabolism.

KEYWORDS: ALTERG; AEROBIC AND ANAEROBIC ENERGY METABOLISM; OXYGEN CONSUMPTION AND LACTATE ACCUMULATION; TIBIAL ACCELERATIONS; INERTIAL MEASUREMENT UNIT

Introduction

Treadmill running under artificial hypogravity has recently entered the focus of sports science and medicine, and gained increasing popularity. Originally offering an alternative training tool for running with reduced musculoskeletal loading in posttraumatic rehabilitation or for injury prevention (Kline et al., 2015), hypogravity running has recently also been employed for competitive training purposes such as supramaximal speed training (Barnes & Janecke, 2017; McNeill, Kline, de Heer, & Coast, 2015). Artificial hypogravity is commonly achieved by specialized instrumented treadmills, which either lift the athlete mechanically (Donelan & Kram, 2000; Polet et al., 2017; Polet, Schroeder, & Bertram, 2018) or by means of positive air pressure inside a chamber around the lower limbs and pelvis of the athlete, lifting the runner upwards. The latter technological concept is known as "lower body positive pressure treadmill" (LBPPT) (Barnes & Janecke, 2017; Kline et al., 2015; McNeill, Kline, et al., 2015) and is applied, e.g., by the commercial product AlterG® Anti-Gravity Treadmill®. On the AlterG®, the effective body weight can be reduced from 100 % down to 20 %, which roughly corresponds to the weight reduction experienced on the Moon. The required positive pressure depends both on the level of unloading and the anthropometry of the runner, and usually ranges between 10 to 100 mbar, thus being uncritical to the human body even in the context of cardiovascular disorders.

While the range of sports employing LBPPT for regular training has become wide, its aim is usually assigned to one of the two categories: (1) increasing running mileage for a prolonged aerobic training stimulus while maintaining a certain upper limit of musculoskeletal loading or (2) increasing running speed while not exceeding individual physiological and/or biomechanical limits in terms of heart rate, oxygen uptake, lactate accumulation or impact loading (Fleckenstein, Ueberschär, Wüstenfeld, & Wolfarth, 2018). In the context of competitive sports, effective body weight is usually reduced to 90 % or 80 % of the original value (e.g.: 630 N or 560 N vs. originally 700 N) but not further, since beyond 80 %, running specificity might be lost because of substantial biomechanical adaptations, such as decreased step frequency etc. (Barnes & Janecke, 2017; Fleckenstein et al., 2018; Kline et al., 2015; Ueberschär, Fleckenstein, Wüstenfeld, et al., 2019).

Detailed research has been conducted to elucidate the physiological adaptations and implications of hypogravity treadmill running (Barnes & Janecke, 2017; Fleckenstein et al., 2018; Kline et al., 2015; McNeill, de Heer, Williams, & Coast, 2015; McNeill, Kline, et al., 2015), confirming that hypogravity running leads to lower physiological demands than running under normal gravity. Thereby, hypogravity allows an athlete either to run faster, or to reduce the physiological session load for a fixed running speed. Only a few studies have addressed biomechanical adaptations to hypogravity running in detail (Barnes & Janecke, 2017; Mercer & Chona, 2015; Moran, Rickert, & Greer, 2017; Ueberschär, Fleckenstein, Wüstenfeld, et al., 2019). Recently, we have shown that LBPPT running does not reduce tibial accelerations as a proxy measure of bone loading (Ueberschär, Fleckenstein, Wüstenfeld, et al., 2019). This counterintuitive result has been confirmed by two other research groups (Mercer & Chona, 2015; Moran et al., 2017). While tibial load stays approximately constant for effective body weight settings of 100 %, 80 % and 60 % at a given running speed, it increases significantly when keeping the physiological demand constant, i.e. when running faster so that a given, e.g. heart rate is achieved. While it is intuitive that running faster, even despite hypogravity conditions, is likely to imply higher tibial accelerations, the question why body-weight unloading does not reduce tibial accelerations for a constant running speed turned out to be challenging. Some authors have hypothesized that a decreased step frequency could nullify a tibial unloading by hypogravity (Moran et al., 2017). However, a thorough investigation of the biomechanics of hypogravity running reveals that this is not fully conclusive in view of the corresponding effect sizes (see below).

Supported by recent research by Polet et al. (Polet et al., 2017, 2018), we were able to explain the counterintuitive findings on non-reduced tibial load in hypogravity from a deductive biomechanical perspective (Ueberschär, Fleckenstein, Wüstenfeld, et al., 2019). Briefly, hypogravity implies a shift in the contributions of vertical and horizontal energy cost of running, i.e. the cyclic work done by the involved muscles to generate propulsion and dynamic balance during stance and at a given running speed (Polet et al., 2017, 2018; Ueberschär, Fleckenstein, Wüstenfeld, et al., 2019). While vertical work is expended for the vertical landing and take-off "collision" interaction of the runner with the ground during stance phase, the major horizontal contribution to total energy cost takes place during swing phase. The latter represents the muscular energy cost for moving the leg forwards during flight phase and comprises the external work done against body segment inertia and internal energy dissipation by frictional losses (Polet et al., 2017, 2018; Ueberschär, Fleckenstein, Wüstenfeld, et al., 2019). At a given gravitational acceleration and running speed, the ratio between vertical and swing phase cost of running seems to be individually optimized to achieve a minimum overall energy expenditure, and thus, to maximize running efficiency (Polet et al., 2017, 2018). Apparently, human motor control is able to (unconsciously) adapt to changes in gravitational acceleration (Polet et al., 2017, 2018; Ueberschär, Fleckenstein, Wüstenfeld, et al., 2019). In case of hypogravity, the contribution of vertical work is reduced to settle to a new energetic optimum, whereby "reduced gravity takes the bounce out of running", as Polet and colleagues illustrated it (Polet et al., 2017, 2018). As a result of that reduced vertical work, the leaps of each step become flatter, i.e. the center of mass exhibits a smaller vertical elevation during flight phase. Intriguingly, this paradoxical implication of hypogravity running could already be observed in video footage of astronauts "walking" and "running" on the Moon, as provided by NASA in the 1960s and 1970s. Notably, this effect is also the dominant reason why tibial load is not diminished or even increased during LBPPT running: Because the parabolic trajectory travelled by the center of mass of the runner is flatter whereas the period of stance phase stays roughly constant, a disproportionately high horizontal take-off velocity must be generated by the runner during the same period of ground contact for achieving the same horizontal running speed. This is only achievable through higher horizontal accelerations. Because the positive pressure effect of LBPPTs only acts vertically, no horizontal support is given. Hence, higher horizontal accelerations must be generated during take-off and absorbed during landing without mediation, resulting in a higher musculoskeletal loading of the lower limbs , manifesting itself in higher tibial accelerations (Ueberschär, Fleckenstein, Wüstenfeld, et al., 2019).

Providing a mathematical foundation, Polet et al. (Polet et al., 2017, 2018) chose the following approximation for the net energy expenditure of running:

$$W_{\text{tot}}^{(\text{net})} = W_{\perp}^{(\text{net})} + W_{\text{swing}}^{(\text{net})} = \tfrac{1}{2} m v_{\perp}^{\,2} + A^{(\text{net})} f^2 \qquad (1)$$

where $W_{\text{tot}}^{(\text{net})}$, $W_{\perp}^{(\text{net})}$ and $W_{\text{swing}}^{(\text{net})}$ denote[1] net total, vertical and swing phase work, respectively. Moreover, m and $v_{\perp}$ are the mass and the vertical take-off speed of the runner. f denotes the frequency of bilateral (i.e. step by step) leg swing and $A^{(\text{net})}$ is a constant net cost parameter being independent of hypogravity (Polet et al., 2017, 2018).

Although representing a simplified concept, Eq. (1) succeeded in explaining most of the biomechanical effects that Polet et al. had observed in their study on a mechanical hypogravity treadmill with ten recreational runners at a jogging speed of 7.2 km h-1 (Polet et al., 2017, 2018).

[1] A complete list of mathematical symbols is given at the end of this article.

However, as the authors did not measure the energy expenditure of the runners and associated costs, the question remains if Eq. (1) describes energy contributions with quantitative accuracy, especially with respect to running speeds of 12–18 km h-1 and beyond, being relevant to competitive distance running and triathlon training. The present study was conducted to answer that question based on 15 well-trained distance runners and triathletes. In addition to verifying Eq. (1), spiroergometric and blood lactate measurements were used to quantify the gross energy cost of hypogravity running on a LBPPT for relevant speeds. Furthermore, the frequency-dependence of the swing phase costs, as characterized by the parameter $A^{(\mathrm{net})}$ in Eq. (1), was studied in detail.

Subjects and methods

Subjects

Fifteen well-trained male runners and triathletes took part (30.2±6.8 years, 72.5±5.1 kg, 181±6 cm, body mass index 22.2±1.5 kg m^{-2}, peak oxygen uptake 60.2±3.8 ml kg^{-1} min^{-1}). The athletes were familiar with treadmill running and all possessed an official personal best of less than 40 min for 10 km road or track running with a mean of 34:06±2:26 min. The study was conducted in accordance with the Declaration of Helsinki. All subjects had given signed written consent prior to their participation.

Treadmill tests

All subjects completed three incremental treadmill tests until volitional exhaustion in randomized order. Two tests were performed on the LBPPT with an effective weights ratio (or "body weight setting" BW_{Set} (Farina, Wright, Ford, Wirfel, & Smoliga, 2017)) of $\gamma = 80$ % and $\gamma = 60$ %, where

$$\gamma \equiv BW_{\mathrm{Set}} := \frac{\text{Effective body weight}}{\text{Standard gravity body weight}} \cdot 100\,\% \leq 100\,\% \qquad (2)$$

The $\gamma = 100$ % (i.e. full weight) test was conducted on a conventional treadmill (h/p/cosmos saturn® 250/100, h/p/cosmos sports & medical GmbH, 83365 Nußdorf – Traunstein, Germany) for ensuring entirely "unaltered" running. Following standard test design from current literature, each test consisted of 3 min stages, each followed by a 30 s break during which capillary blood was taken (Barnes & Kilding, 2015; R. Beneke & Leithäuser, 2017; Bentley, Newell, & Bishop, 2007). The initial running speed was set to 6 km h^{-1} and increased by 2 km h^{-1} after each stage. During each test, the first three stages (i.e., 6 –10 km h^{-1}) were used as a standardized warm-up. Further, regarding all three tests, the participants successfully completed stages 1–7 (i.e., 6–18 km h^{-1}). In addition, the stages 8–9 (i.e., 20–22 km h^{-1}) were completed by all 15 runners for the hypogravity conditions of $\gamma = 80$ % and 60 %. Although the majority of subjects completed further stages, those data were disregarded to ensure an identical cohort of subjects for all gravity conditions and speed stages.

During all tests, the subjects wore the same individual pair of shoes to exclude footwear-related effects (Hollander, Riebe, Campe, Braumann, & Zech, 2014; Squadrone & Gallozzi, 2009). For a given subject, all tests were conducted on the same day and at the same time with one week between each test. For standardizing test conditions, the subjects agreed to adopt similar training loads before the tests, including a rest period with no training one day before, and to follow similar nutrition patterns for at least two days in advance.

Lower body positive pressure treadmill

For hypogravity running, the motorized LBPPT AlterG® Anti-Gravity Treadmill® (Pro 200 Plus, AlterG®, Fremont, California, USA) was used. Its working principle has been outlined above: Due to a slight positive pressure p_i inside the lower-body chamber with a difference of $\Delta p := p_i - p_0 \approx 10...100\,\text{mbar}$ to external standard pressure of $p_0 \approx 1000\,\text{mbar}$, a pressure gradient force $\vec{F}_{\Delta p}$ vertically lifts the runner, thereby reducing the acting gravitational force $\vec{F}_G$ by $\vec{F}_{\Delta p}$ (Figure 1 (a)):

$$\vec{F}_{G,\,\text{eff}} = \vec{F}_G + \vec{F}_{\Delta p} = -mg_0\vec{e}_z + \Delta p\, A_{\text{ath}}\vec{e}_z = -mg_0\left(1 - \frac{\Delta p\, A_{\text{ath}}}{mg_0}\right)\vec{e}_z = -mg_0\gamma\vec{e}_z \qquad (3)$$

Here, $\vec{F}_G = -mg_0\vec{e}_z$ denotes the standard gravitational force with the athlete's mass m, the gravitational acceleration constant $g_0 = 9.80665\,\text{m s}^{-2}$ and the unit vector $\vec{e}_z$ of the vertical z axis (in the global laboratory coordinate system, i.e. pointing upwards), while A_{ath} is the athlete's cross-sectional area at the LBPPT chamber girdle around the upper lumbar spine region (cf. Figure 1 (a)). As suggested by the last term of Eq. (3), the effective weight force $\vec{F}_{G,\,\text{eff}}$ can be expressed in analogy to $\vec{F}_G = mg_0$ by using the effective weight ratio γ from Eq. (2) and introducing an effective gravitational acceleration $g := \gamma g_0 < g_0$, reading $\vec{F}_{G,\,\text{eff}} = -mg\vec{e}_z = \gamma\vec{F}_G$. For the used LBPPT, the unloading coefficient $\gamma \equiv g/g_0$ can be continuously set between 100 % down to 20 %. Notably, even though the athletes' effective weights are altered by the positive pressure effect, their masses stay constant, as required by the basic physical principle of mass conservation. Hence, inertial forces will remain unaffected by hypogravity.

Tibial inertial measurement units

For detecting impact events, two inertial measurement units (IMUs; Xsens Technologies B.V., MTw Awinda, Enschede, Netherlands) were fixed anteromedially at the distal tibiae using tightly fitting Velco™ straps (Figure 1 (b)). Details of that measurement system and its application for assessing tibial acceleration loads have been described before (Ueberschär, Fleckenstein, Warschun, Kränzer, et al., 2019). The lightweight sensors (16 grams, 4.7 cm · 3.0 cm · 1.3 cm) measure 3D accelerations within a range of $\pm 16g_0$ for each spatial axis at an internal sampling rate of 1,000 Hz. The output rate (after sensor fusion) was set to 120 Hz. Their suitability and validity for assessing lower limb biomechanics during running was shown by previous studies (Hamacher, Hamacher, Taylor, Singh, & Schega, 2014; A. Karatsidis et al., 2016; Angelos Karatsidis et al., 2018; Munoz Diaz, Kaiser, & Bousdar Ahmed, 2018; Ueberschär, Fleckenstein, Warschun, Kränzer, et al., 2019; Ueberschär, Fleckenstein, Warschun, Walter, & Hoppe, 2019).

Spirometry and lactate measurements

Spirometric data (i.e., oxygen intake, carbon dioxide output and minute ventilation) were acquired throughout all speed stages and breaks between the stages using a stationary breath-by-breath system (Quark CPET, COSMED, Pavona di Albano, Italy), and processed afterwards by the software OMNIA 1.6 (COSMED, Pavona di Albano, Italy). Additionally, heart rates were recorded via chest belts using short-range telemetry (HRM Run™, Garmin Ltd., Canton Schaffhausen, Switzerland). Between the speed stages, directly after as well as 3 and 5 min after test termination, 20 µl of capillary blood samples were taken from the earlobe, solubilized in a

1,000 µl hemolysate solution and analyzed for their lactate concentration using the SUPER GL ambulance device (Dr. Müller Gerätebau GmbH, Freital, Germany). Finally, the subjective rating of perceived exertion was assessed after each stage and after termination using the Borg scale (Borg, 1970).

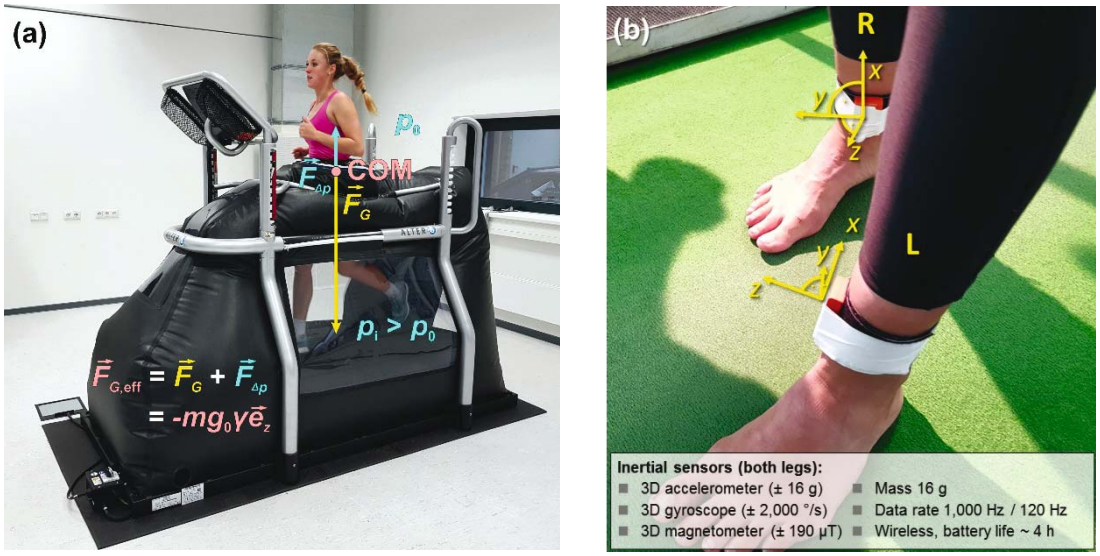

Figure 1. Measurement setup. The employed hypogravity treadmill AlterG® and tibial inertial measurement units. (a) Schematic diagram of the lower body positive pressure treadmill unloading principle: By the positive air pressure difference $\Delta p = p_i - p_0 > 0$ between inside and outside the LBPPT chamber (black), a positive pressure gradient force $\vec{F}_{\Delta p} = +\Delta p\, A_{\mathrm{ath}}\vec{e}_z$ acts on the center of mass (COM) of the athlete in opposite direction as gravity $\vec{F}_G = -m\, g_0\vec{e}_z$, resulting in a reduced effective weight force $\vec{F}_{G,\mathrm{eff}} = -mg_0\gamma\vec{e}_z$ (see text). For simplicity, the marginal secondary torques resulting from non-coinciding force application points of gravity and buoyancy are disregarded in this simplified sketch. (b) Inertial measurement units fixed anteromedially at the distal tibiae of the runners to measure tibial accelerations.

Data processing

Physiological data

Gross total energy expenditure[2] (W_{tot}, $[W_{\mathrm{tot}}] = \mathrm{J}$) during exercise is the sum of the aerobic ($W_{\dot{V}_{O_2}}$), anaerobic lactic (W_{La}) and anaerobic alactic contributions (W_{CP}): $W_{\mathrm{tot}} = W_{\dot{V}_{O_2}} + W_{\mathrm{La}} + W_{\mathrm{CP}}$ (Ralph Beneke & Hütler, 2005; R. Beneke & Leithäuser, 2017; Shaw, Ingham, & Folland, 2014; Zagatto, Leite, Papoti, & Beneke, 2016). For steady-state conditions during cyclic running, the anaerobic alactic contribution of creatine phosphate $W_{\mathrm{CP}} \approx W_{\dot{V}_{O_2}}$ is negligible, so that $W_{\mathrm{tot}} \approx W_{\dot{V}_{O_2}} + W_{\mathrm{La}}$ (Barnes & Kilding, 2015; R. Beneke & Leithäuser, 2017). To compute energy costs, total energy expenditure and its aerobic and anaerobic contributions were normalized by body mass m and number of steps $n \approx 1$, yielding the total energy cost per step

[2] Note that in contrast to the net quantities in Eq. (1), no superscript is used for gross work symbols throughout this article for the sake of clarity.

$$W'_{\mathrm{tot}} \approx W'_{\dot{V}_{\mathrm{O}_2}} + W'_{\mathrm{La}} \tag{4}$$

with $W'_{\mathrm{tot}} \equiv W_{\mathrm{tot}} / (m \cdot n)$ and $\left[W'_{\mathrm{tot}}\right] \equiv \mathrm{J\ kg^{-1}}$ etc. Dividing Eq. (4) by the individual step period $T_{\mathrm{step}} = \frac{1}{2} T_{\mathrm{stride}}$ (where T_{stride} denotes the stride period), the equivalent relation $\frac{1}{T_{\mathrm{step}}} W'_{\mathrm{tot}} \approx \frac{1}{T_{\mathrm{step}}} W'_{\dot{V}_{\mathrm{O}_2}} + \frac{1}{T_{\mathrm{step}}} W'_{\mathrm{La}}$ for mass-normalized mechanical power (units $\left[\frac{1}{T_{\mathrm{step}}} W'_{\mathrm{tot}}\right] = \mathrm{W\ kg^{-1}}$ was obtained. The aerobic and anaerobic lactic contributions to gross power were approximated as functions of the mass-normalized oxygen uptake $\dot{V}'_{\mathrm{O}_2} = \dot{V}_{\mathrm{O}_2} / m$ ($\left[\dot{V}'_{\mathrm{O}_2}\right] = \mathrm{ml\ min^{-1}\ kg^{-1}}$), respiratory quotient $RQ = \dot{V}_{\mathrm{CO}_2} / \dot{V}_{\mathrm{O}_2}$ ($[RQ] = 1$) and change in blood lactate concentration with respect to previous running speed Δc_{La} ($\left[\Delta c_{\mathrm{La}}\right] = \mathrm{mmol\ ml^{-1}}$) as follows (Barnes & Kilding, 2015; Ralph Beneke, Beyer, Jachner, Erasmus, & Hütler, 2004; R. Beneke & Leithäuser, 2017; di Prampero, 1981; Lacour & Bourdin, 2015; Lusk, 1924):

$$\frac{1}{T_{\mathrm{step}}} W'_{\dot{V}_{\mathrm{O}_2}} \left(\dot{V}'_{\mathrm{O}_2}, RQ\right) \approx \left(\dot{V}'_{\mathrm{O}_2} - 4.5 \frac{\mathrm{ml}}{\mathrm{kg\ min}}\right) \cdot \left(15.974 + 5.157 \cdot RQ\right) \frac{\mathrm{J}}{\mathrm{ml}}, \tag{5}$$

$$\frac{1}{T_{\mathrm{step}}} W'_{\mathrm{La}} \left(\Delta c_{\mathrm{La}}\right) \approx \Delta c_{\mathrm{La}} \cdot 3.0 \frac{\mathrm{ml}}{\mathrm{kg\ min\ mmol\ l^{-1}}} \cdot 21.131 \frac{\mathrm{J}}{\mathrm{ml}}. \tag{6}$$

In Eq. (5), a rough approximation of the resting oxygen uptake of 4.5 ml $\mathrm{kg^{-1}}$ $\mathrm{min^{-1}}$ for standing still was presumed as regards the aerobic contribution, while for the anaerobic lactic contribution in Eq. (6), a lactate oxygen equivalent of 3.0 ml $\mathrm{kg^{-1}}$ $\mathrm{min^{-1}}$ oxygen uptake per 1 mmol $\mathrm{l^{-1}}$ increase in lactate concentration was used (R. Beneke & Leithäuser, 2017; Lacour & Bourdin, 2015). A negative change in lactate concentration from stage to stage, i.e. $\Delta c_{\mathrm{La}} < 0$, reflects an oxidative degradation of lactate, i.e. a lactate-based aerobic energy expenditure. In that case, the lactic anaerobic contribution was considered 0 in Eq. (6), while the (small) additional aerobic contribution by lactate oxidation was roughly covered by Eq. (5). To calculate energy costs per step, Eq.(4)–(6) were evaluated for each athlete, gravity condition and running speed using Microsoft Excel 2016 (Microsoft Corporation, Redmond, USA) and Origin 2017 (OriginLab Corp., Massachusetts, USA).

Biomechanical data

The temporal structure of the running cycles was determined based on the 3D accelerations $\vec{a} = \left(a_x, a_y, a_z\right)^{\mathrm{T}}$ of the distal tibiae as measured by the IMUs. Based on the mean time series of the acceleration magnitude, i.e. $a = \sqrt{a_x^{\,2} + a_y^{\,2} + a_z^{\,3}}$, key events were detected by a self-made software (LabVIEW 2016 64 bit, National Instruments, Austin, Texas, USA) (Ueberschär, Fleckenstein, Warschun, Kränzer, et al., 2019). First, the overall peaks in acceleration per step (Figure 2: red upper triangles) were detected, reflecting the moment of maximum impact and active acceleration during ground contact. Those events were easily and robustly detected due to their dominance in the time series. In addition, the first minimum value before such an impact peak (Figure 2: squares) was identified as the moment of initial ground contact, i.e. the start of stance phase (Strohrmann, Harms, Kappeler-Setz, & Troster, 2012). Conversely, the end of stance phase was approximated by the first major peak (Figure 2: circles) succeeding the main impact peak, as confirmed in a pilot study by comparing to ground reaction forces. The detection of that second peak requires more sensitive algorithms, since it is sometimes preceded by another minor peak, as observable in Figure 2, the latter probably reflecting a segmental lift-off of the

foot. Hence, the automatic detection of stance phase end was automatically checked for plausibility and, in case of questionable results, manually by an experienced researcher. Notably, the described procedure refines the approach of Strohrmann et al. (Strohrmann et al., 2012), who approximated the end of the stance phase by the moment when tibial acceleration exceeded a constant threshold of $2g_0$ after the main impact peak, which is apparently not applicable to the gait structure of the competitive athletes of this study.

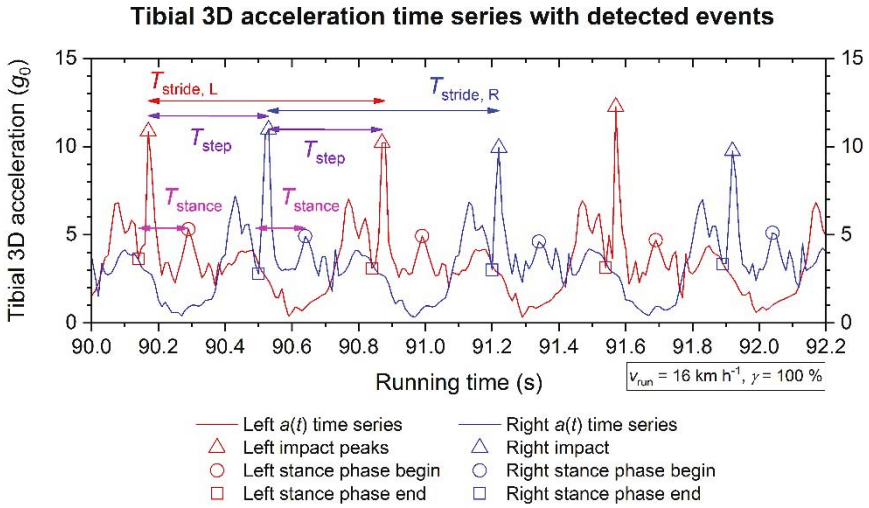

Figure 2. Sample of acquired tibial acceleration data with detected events. Key events in 3D tibial acceleration magnitude (left: red, right: blue) were automatically detected by a dedicated LabVIEW program, comprising main impact peak (upper triangles), start of stance phase (squares) and end of stance phase (circles). Based on those events, stride, step and stance periods T_{stride}, T_{step} and T_{stance} were calculated.

Because no subject exhibited any pronounced lateral asymmetries in step cycle timing or peak impact acceleration for the speed stages and gravity conditions studied, the mean values of step periods and peak tibial impact accelerations of the left and right leg were used for simplicity.

Following point mass physics of the athlete's COM (while the damping effect of the LBPPT belt is considered negligible), vertical take-off velocity $v_\perp$ was calculated for a given gravity level γ and running speed v_{run} according to

$$v_\perp = \tfrac{1}{2}\left(T_{\text{step}} - T_{\text{stance}}\right) g = \tfrac{1}{2}\left(\tfrac{1}{2} T_{\text{stride}} - T_{\text{stance}}\right) \gamma g_0 \tag{7}$$

based on the values of detected mean stride and stance periods $T_{\text{stride}} = 2T_{\text{step}}$ and T_{stance}, respectively. Furthermore, step length $s_{\text{step}} \equiv \tfrac{1}{2} s_{\text{stride}}$, i.e. half stride length, was calculated based on $v_\perp$ and v_{run} via

$$s_{\text{step}} = \frac{2v_\perp}{\gamma g_0} v_{\text{run}} \tag{8}$$

Knowing energy costs per step from Eq. (4)–(6) and step length from Eq. (8), energy costs per meter were calculated as

$$W''_{\text{tot}} = \frac{W'_{\text{tot}}}{s_{\text{step}}} = \frac{W'_{\dot{V}_{O_2}}}{s_{\text{step}}} + \frac{W'_{\text{La}}}{s_{\text{step}}} = W''_{\dot{V}_{O_2}} + W''_{\text{La}} \tag{9}$$

with units $\left[W''_{\text{tot}}\right] = \left[W''_{\dot{V}_{O_2}}\right] = \left[W''_{\text{La}}\right] = \text{J m}^{-1}$. Furthermore, the ratio of gross vertical vs. gross swing

phase cost was calculated from total energy cost per step and vertical take-off speed using Eq. (1) :

$$\frac{W'_{\perp}}{W'_{\text{swing}}} = \frac{\eta^{-1}\,\frac{1}{2}v_{\perp}^{\,2}}{W'_{\text{tot}} - \eta^{-1}\,\frac{1}{2}v_{\perp}^{\,2}} \tag{10}$$

Here, the efficiency $\eta \equiv W_{\perp}^{(\text{net})}/W_{\perp}$ denotes the ratio of net vs. gross vertical work. For walking and running, it comprises both the positive elevation work for accelerating upwards and the "negative work" work required for decelerating at landing in each step cycle (Margaria, 1968; Minetti, Moia, Roi, Susta, & Ferretti, 2002). Both actions require a positive muscular energy expenditure, while the net gain and loss in potential energy (via vertical kinetic energy) compensate for each other due to cyclicity (Margaria, 1968; Minetti et al., 2002). Magaria experimentally derived a value of $\eta \approx 0.207$ as the result of the reciprocal sum of concentric muscular action during positive work ($\eta_{\text{con}} \approx 0.25$) and eccentric action during negative work ($\eta_{\text{ecc}} \approx -1.2$), i.e. $\eta^{-1} = {\eta_{\text{con}}}^{-1} + {\eta_{\text{ecc}}}^{-1} = (0.25)^{-1} + \left(-(-1.2)^{-1}\right) \approx (0.207)^{-1}$, which was later principally confirmed by experiments of Minetti et al. (Margaria, 1968; Minetti et al., 2002).

Statistical analysis

All statistical analyses were conducted with IBM SPSS Statistics 23 (IBM, Armonk, USA). If not stated otherwise, all results are given as mean ± standard deviation (SD) in the text. In the graphs, data points and error bars depict mean $\pm 1.96\,SE = 1.96/\left(\sqrt{15}\,SD\right) \approx 0.5\,SD$, where SE denotes the standard error. By that choice, the error probability, i.e. the statistical probability that the real value does not fall within the given range, is $p < 0.05$. For significance tests, if not stated otherwise, a univariate two-way analysis of variance (ANOVA) with repeated measures was conducted for the main factors gravity level γ and running speed v_{run}. Pairwise post-hoc tests were performed with Bonferroni correction. Standard level of significance was set to $p < 0.05$. Effect sizes were interpreted, where relevant, based on partial ${\eta_{\text{partial}}}^2$ according to Cohen (Cohen, 1973; Richardson, 2011).

Results

Step and stance periods

Regarding step and stance periods, the results are presented as a function of gravity level and running speed in Figure 3. For step period, a significant increase with lower gravity levels γ was found ($p < 0.001$). For stance period, however, differences appeared stochastic within measurement uncertainty and proved insignificant among gravity conditions, so that the mean for all three gravity levels γ is shown (magenta data points). As regards speed dependence, both step and stance period exhibit a decrease with increasing running speed ($p < 0.001$). Linear fits

$$T_{\text{step}} = T_{\text{step}}^{(0)} - \delta_{\text{step}} \cdot v_{\text{run}} \tag{11}$$

provide high adjusted coefficients of determination (Figure 3) and yield $T_{\text{step}}^{(0)} = 435\pm7,\ 438\pm2,\ 458\pm1$ ms as well as $\delta_{\text{step}} = 5.66\pm0.05,\ 5.26\pm0.02,\ 5.6\pm0.01$ ms $\left(\text{km h}^{-1}\right)^{-1}$ for $\gamma = 100$ %, 80 % and 60 %, respectively. Also for stance period, linear fits confirm an analogously deceasing trend $T_{\text{stance}} = T_{\text{stance}}^{(0)} - \delta_{\text{stance}} \cdot v_{\text{run}}$ with $T_{\text{stance}}^{(0)} = 184 \pm 8$ ms and $\delta_{\text{stance}} = 1.3 \pm 0.5$ ms$\left(\text{km h}^{-1}\right)^{-1}$, while the

achieved portion of variance explained is lower ($\overline{R}^2 \approx 0.63$, Figure 3).

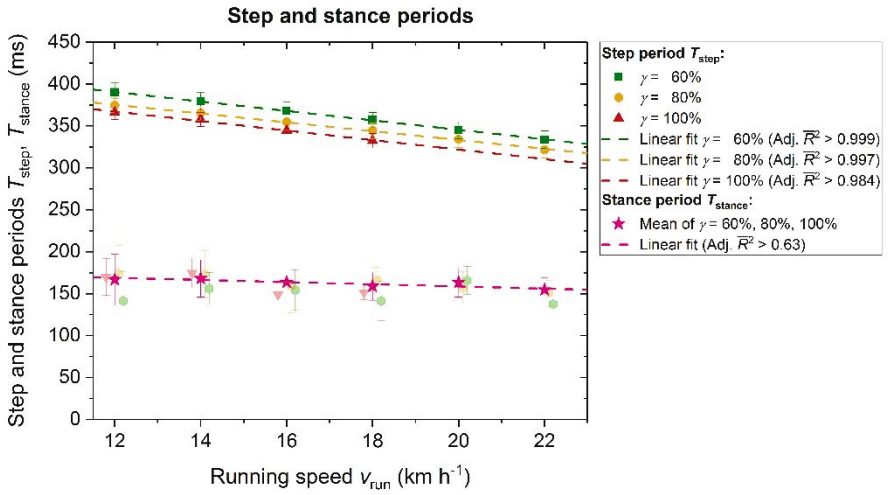

Figure 3. Step and stance periods. Colors indicate the gravity level γ. Note that for stance periods, the data points for $\gamma = 60$ %, 80 % and 100 % are slightly horizontally stacked for reasons of clarity.

Vertical take-off speed, flight height and step length

In Figure 4 (a), the relation between vertical take-off speed and running speed is shown for the different gravity conditions. Irrespective of gravity level, vertical take-off speed significantly reduces with increasing running speed ($p < 0.001$; pairwise post-hoc Bonferroni $p < 0.02$ except for 20 vs. 22 km h^{-1}). Notably, for a given running speed, hypogravity induces a significant *reduction* in vertical take-off speed ($p < 0.001$). A linear dependence well describes the experimental findings, best fits

$$v_{\perp} = \alpha + \beta v_{\text{run}} \tag{12}$$

yielding $\alpha = 1.229 \pm 0.031$ m s^{-1}; $\beta = -0.0060 \pm 0.0006$ for $\gamma = 100\%$ ($\overline{R}^2 > 0.973$), $\alpha = 0.996 \pm 0.008$ m s^{-1}; $\beta = -0.0043 \pm 0.0001$ for $\gamma = 80\%$ ($\overline{R}^2 > 0.995$) and $\alpha = 0.805 \pm 0.002$ m s^{-1}; $\beta = -0.0035 \pm 0.0001$ for $\gamma = 60\%$ ($\overline{R}^2 > 0.999$), respectively.

In Figure 4 (b), the flight height, i.e. the vertical distance travelled upwards by the runner's during flight phase, is shown as a function of step length. For all gravity conditions, step length significantly grew with running speed ($p < 0.001$; pairwise post-hoc Bonferroni $p < 0.001$ for all speed differences ≥ 4 km h^{-1}), and, in turn, flight height reduced with step length as running speed increases. For a given running speed, flight height became significantly *smaller* for a higher level of hypogravity unloading, i.e. smaller γ ($p < 0.001$). Interestingly, all ratios of flight height vs. step length seem to roughly follow a common linear dependence, irrespective of the hypogravity condition. Both a square fit and a linear fit practically yield a linear relation, depicted as a blue line in Figure 4 (b):

$$h_{\text{flight}} = 0.0774 \pm 0.0038 - (0.0496 \pm 0.0041)\, s_{\text{step}} \tag{13}$$

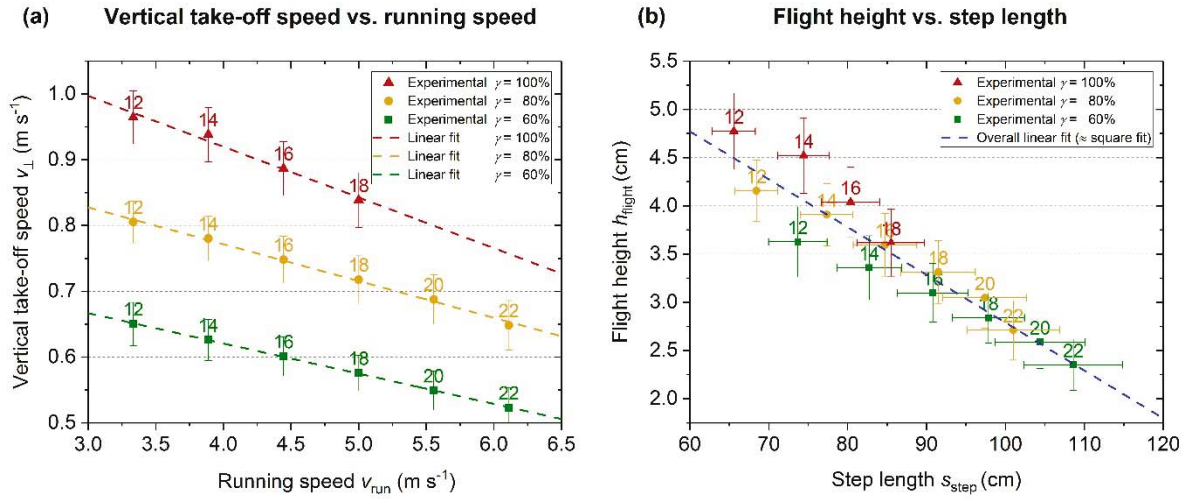

Figure 4. Vertical take-off vs. horizontal running speed. (a) Vertical take-off speed as a function of gravity level (colors) and running speed. (b) Flight height as a function of gravity level and step length. Dotted lines depict the linear fits described in the text.

Energy costs per step

Considering energy cost per step, experimental results for the three gravity conditions and running speeds are summarized in Figure 5. As observed in Figure 5 (a), energy cost per step W'_{tot} significantly grew with higher running speeds for all hypogravity conditions ($p < 0.001$; pairwise post-hoc Bonferroni $p < 0.01$ except for 18 vs. 20 vs. 22 km h^{-1}). As regards the effect of hypogravity, total energy cost per step reduced with decreasing gravity level γ for a given running speed ($p < 0.001$). In Figure 5 (b), energy cost per step is displayed as a function of vertical take-off speed. In both panels (a) and (b) of Figure 5, the experimental data is additionally compared to the fixed-value predictions of the biomechanical model derived below (dotted lines). Without any additional fitting, apparently good agreement was achieved (root mean square (RMS) deviation of 2.9 %). In terms of gross mechanical power, the average energy cost per step at full gravity level $\gamma = 100$ % and a running speed of 16 km h^{-1} amounts to 6.6±0.6 J kg^{-1} and corresponds to approximately 19.1±1.7 W kg^{-1}, i.e. 1335±122 W for a 70 kg runner.

Energy costs per meter

Total energy costs per meter W''_{tot} (Eq. (9)) are plotted in Figure 6 (a) as a function of gravity level and running speed (filled symbols) and compared to their aerobic contribution $W''_{\dot{V}_{O_2}}$ (empty symbols). Both total energy cost per step W''_{tot} and the aerobic component $W''_{\dot{V}_{O_2}}$ significantly reduced with lower gravity levels γ ($p < 0.001$; large effects with ${\eta_{partial}}^2 \approx 0.623$ and 0.645, respectively). Notably, for all hypogravity conditions, total energy cost per meter increased with running speed, yet with a comparably small effect size of ${\eta_{partial}}^2 \approx 0.067$ ($p < 0.009$; pairwise post-hoc Bonferroni tests showed non-significance), whereas the aerobic fraction $W''_{\dot{V}_{O_2}}$ stayed approximately constant ($p > 0.99$, ${\eta_{partial}}^2 \approx 0.001$). That increase was also predicted by the fixed-value biomechanical model (dotted lines in Figure 6 (a)), which matched experimental results convincingly (RMS deviation of 7.7 %). The presumably causal link between the onset of

substantial anaerobic lactic contributions W''_{La} to total energy costs per meter at approximately 16 km h^{-1} for $\gamma = 100$ % and 18 km h^{-1} for $\gamma = 80$ % and 60 % is well observed also in Figure 6 (b). There, the coincidence of the increase in total energy costs and the indication of anaerobic metabolism is highlighted by the significant decrease in the ratio $W''_{\dot{V}_{\mathrm{O_2}}} / W''_{\mathrm{tot}}$ of aerobic to total costs as a function of running speed ($p < 0.001$).

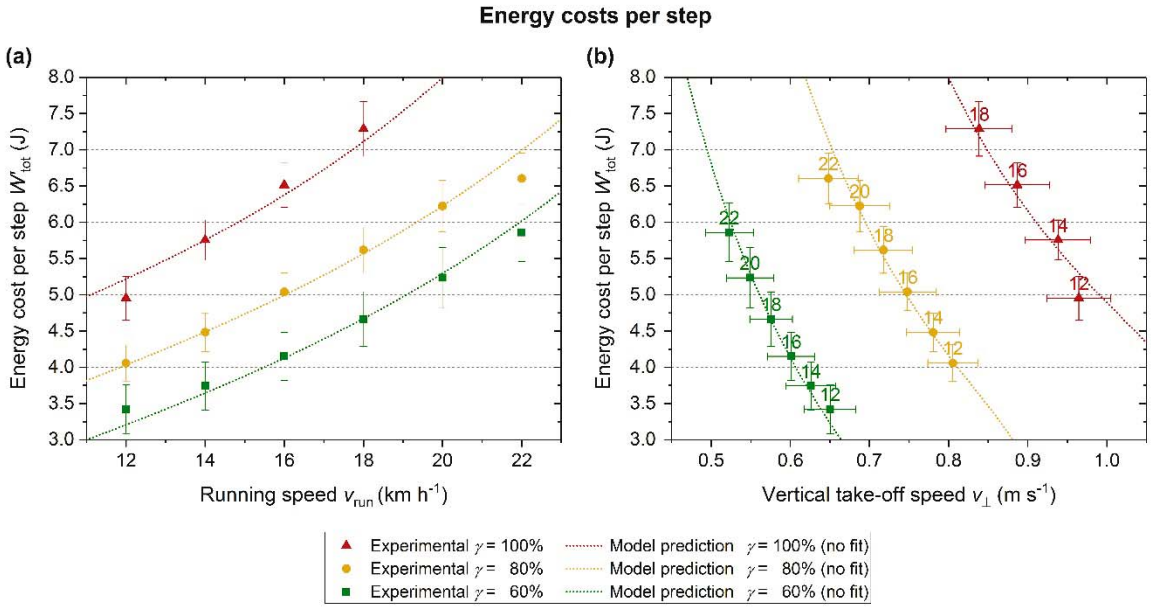

Figure 5. Total energy costs per step. (a) Total energy cost W'_{tot} as a function of gravity level (colors) and running speed. (b) As a function of gravity level and vertical take-off speed. Numerical labels on the data points denote corresponding running speeds. In both panels, dotted lines depict the fixed-parameter model prediction derived below; no additional numerical fitting was done.

Vertical vs. swing phase costs per step

As for the ratio of vertical vs. swing phase costs per step $W'_{\perp} / W'_{\mathrm{swing}}$, results are presented in Figure 7 (a) and (b) as functions of running speed and vertical take-off speed, respectively. Two major effects were observed, confirming and extending the findings on total energy costs per step: For a given running speed, the ratio of vertical vs. swing phase cost reduced with decreasing gravity level ($p < 0.001$). Second, vertical energy cost per step $W'_{\perp}$ was significantly attenuated at smaller running speeds for all gravity conditions ($p < 0.001$, pairwise post-hoc Bonferroni $p < 0.02$ except for 18 vs. 20 and 20 vs. 22 km h^{-1}). Fixed-value model predictions again matched well the experimental results (RMS deviation of 5.8 %).

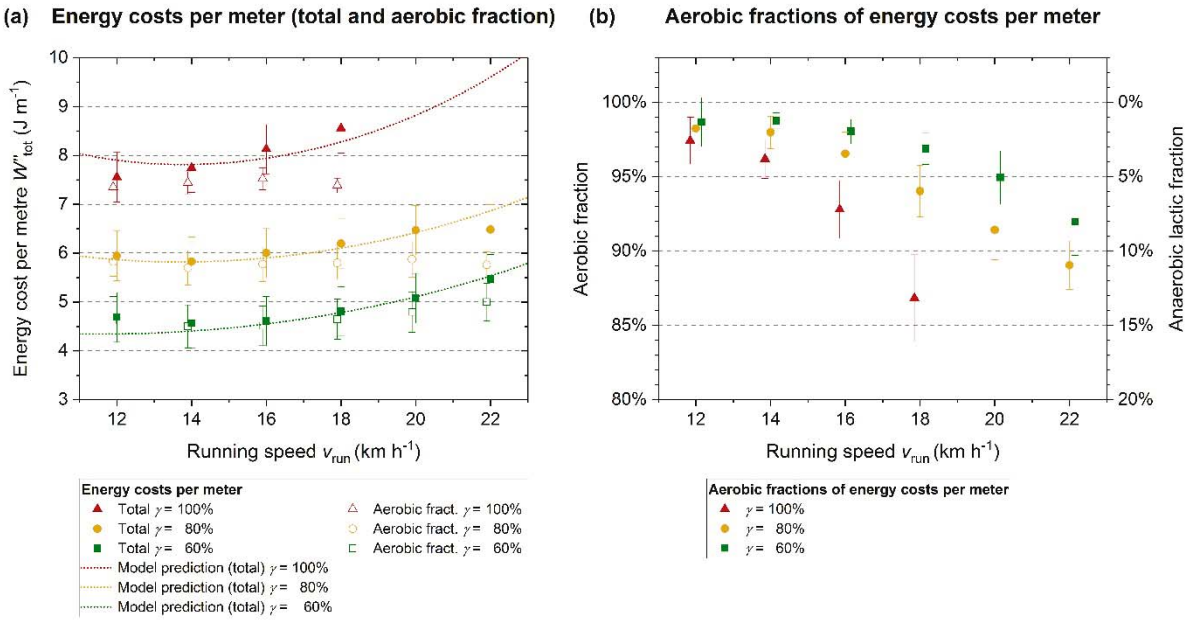

Figure 6. Total energy costs per meter and their aerobic fraction. (a) Energy costs per meter (filled symbols: total W''_{tot}; empty symbols: aerobic contribution $W''_{\dot{V}_{O_2}}$) in Joules per meter along with model predictions (dotted lines, not additional fits). (b) Percentage $W''_{\dot{V}_{O_2}} / W''_{tot}$ of aerobic contribution vs. total energy costs per meter. Note that for reasons of clarity, symbols have been slightly horizontally stacked to avoid overlapping in panel (b).

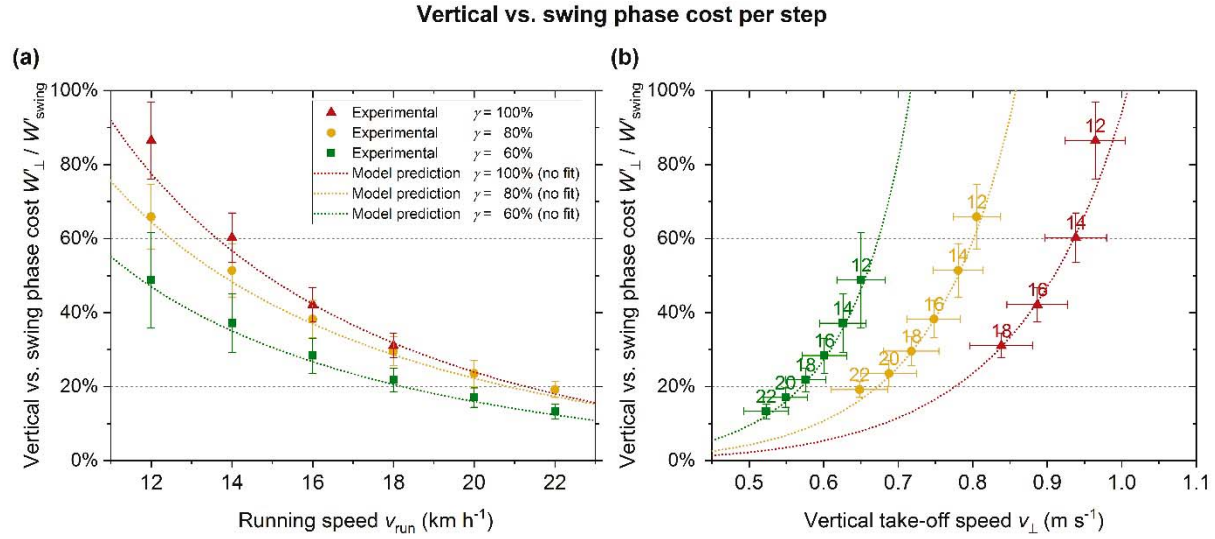

Figure 7. Ratio of vertical vs. swing phase cost per step. (a) Cost ratio $W'_{\perp}/W'_{swing}$ as a function of running speed. (b) As a function of vertical take-off speed. Numerical labels denote corresponding running speeds (in km h^{-1}), while dotted lines depict the fixed-parameter model prediction without additional numerical fitting.

Model enhancement

In the following, the model of Polet et al. is enhanced and refined on the basis of the experimental results presented above. Reformulating Eq. (1) for gross quantities using the nomenclature of this study and bilateral (i.e. step by step) flight time T_{flight}, energy cost per step and kilogram

body weight can be expressed as

$$W'_{\mathrm{tot}} = \tfrac{1}{2}\eta^{-1}v_{\perp}{}^{2} + \frac{A}{T_{\mathrm{flight}}{}^{2}} \tag{14}$$

where $T_{\mathrm{flight}} \equiv f^{-1} = T_{\mathrm{step}} - T_{\mathrm{stance}} = \tfrac{1}{2}T_{\mathrm{stride}} - T_{\mathrm{stance}}$ denotes the bilateral flight time and A the gross swing phase cost parameter (units $[A] = \mathrm{J\ kg^{-1}\ Hz^{-2}} \equiv \mathrm{m^2}$). A from Eq. (14) is related to the corresponding net cost parameter $A^{(\mathrm{net})}$ from Eq. (1) via

$$A = \frac{A^{(\mathrm{net})}}{m \cdot \eta_{\mathrm{swing}}} \tag{15}$$

where m is the mass of the runner and η_{swing} the (unknown) efficiency of swing phase muscular work. Inserting Eq. (7) into Eq. (14) yields a total energy cost per step of

$$W'_{\mathrm{tot}} = \tfrac{1}{2}\eta^{-1}v_{\perp}{}^{2} + \frac{4A\gamma^{2}g_{0}{}^{2}}{v_{\perp}{}^{2}} \tag{16}$$

and, via Eq. (9) and (8) a total energy cost per meter of

$$W''_{\mathrm{tot}} = \tfrac{1}{4}\eta^{-1}\gamma g_{0}\frac{v_{\perp}}{v_{\mathrm{run}}} + \frac{2A\gamma^{3}g_{0}{}^{3}}{v_{\perp}{}^{3}v_{\mathrm{run}}} \tag{17}$$

Polet et al. considered a constant running speed of $v_{\mathrm{run}} = 7.2$ km h^{-1}, and thus were able to assume a constant individual value for $A = \mathrm{const}$. Hence, the swing phase cost did not depend on the gravity level, i.e. $\partial A/\partial\gamma = 0$. According to our experimental data, as presented in Figure 8, this assumption cannot be upheld for the running speeds studied here: A small but distinct difference between the hypogravity levels $\gamma = 80$ % and 60 % was observed, while a substantial difference was observed for $\gamma = 100$ %. The latter deviation likely represents an aggregated result of the absence of hypogravity unloading *and* the absence of the LBPPT chamber girdle, which presumably exerts a non-vanishing base level of unloading support as compared to standard treadmill running.

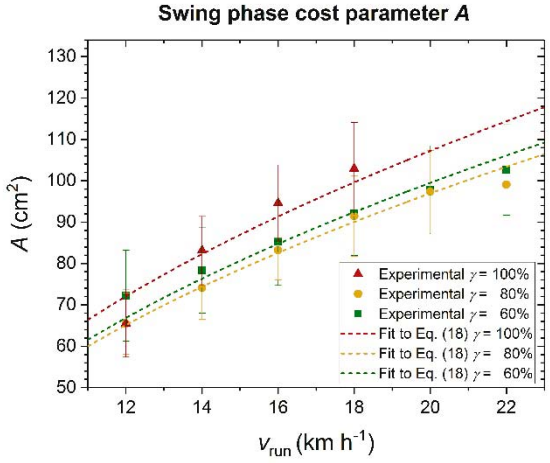

Figure 8. Swing phase cost parameter A. Dashed lines depict fits to Eq. (18).In view of the data down in Figure 8, we extend the model of Polet et al. by introducing a dependence on gravity level and a running speed by proposing

$$A(\gamma, v_{\text{run}}) = \zeta(\gamma)\sqrt{\frac{v_{\text{run}} - v_0}{v_0}} \tag{18}$$

Best fits of the experimental data to Eq. (18) with a common "minimal" running speed v_0 and a gravity-dependent scaling factor $\zeta(\gamma)$ ($[\zeta] = [A] = \text{m}^2$) yield a total adjusted coefficient of determination of $\overline{R}^2 \approx 0.95$. The scaling factors are $\zeta(\gamma) = 65\pm7$, 60 ± 6 and 61 ± 6 cm^2 for $\gamma =$ 100 %, 80 % and 60 %, respectively, while the common minimum speed amounts to $v_0 = 5.4 \pm 0.7$ km h^{-1} Physiologically, this hypogravity-independent, non-zero offset seems to reflect a base line of required muscular energy cost for swing phase, probably corresponding to the energetic cost of thigh and shank pendulum motion and counterbalancing work in the trunk and upper limbs, including several large muscle groups. Using Eq. (16), (18) and (12), the total energetic cost per step can be expressed as a function of gravity and running speed, yielding

$$W'_{\text{tot}}(\gamma, v_{\text{run}}) = \tfrac{1}{2}\eta^{-1}\left(\alpha(\gamma) + \beta(\gamma)v_{\text{run}}\right)^2 + \frac{\zeta(\gamma)\sqrt{v_{\text{run}}/v_0 - 1}}{\left(\alpha(\gamma) + \beta(\gamma)v_{\text{run}}\right)^2} \tag{19}$$

The prediction of Eq. (19) as shown in Figure 5 (a) matches well the experimental data. Regarding energetic cost per step as a function of vertical take-off velocity, Eq. (19) can be rewritten using Eq. (12), yielding

$$W'_{\text{tot}}(\gamma, v_\perp) = \tfrac{1}{2}\eta^{-1}{v_\perp}^2 + \frac{4\gamma^2 {g_0}^2 \zeta(\gamma)}{{v_\perp}^2}\sqrt{\frac{v_\perp - \alpha(\gamma)}{\beta(\gamma)v_0} - 1} \tag{20}$$

As discussed in the context of Figure 5 (b), also this prediction shows good agreement with experimental data. Moreover, the cost ratios of vertical vs. swing work can be expressed using Eq. (16), resulting in

$$\frac{W'_\perp}{W'_{\text{swing}}} = \frac{\eta^{-1}{v_\perp}^4}{8A{g_0}^2\gamma^2} = \frac{{v_\perp}^4}{8\eta{g_0}^2\gamma^2\zeta(\gamma)}\left(\frac{v_\perp - \alpha(\gamma)}{\beta(\gamma)v_0} - 1\right)^{-1/2} = \frac{\left(\alpha(\gamma) + \beta(\gamma)v_{\text{run}}\right)^4}{8\eta{g_0}^2\gamma^2\zeta(\gamma)\sqrt{v_\perp/v_0 - 1}} \tag{21}$$

as depicted in Figure 7 (a) as a function of γ and v_{run}, and in (b) as a function of γ and $v_\perp$, respectively. As before, the degree of correspondence between experimental data and the model prediction is high.

Discussion

This study has yielded five key findings on treadmill running in hypogravity. First, as for *temporal gait structure*, step periods decreased with increasing running speed for all gravity conditions, the average drop amounting to -6 ms (i.e. ≈ -1.6 %) per +1 km h^{-1} increase in running speed. Step periods also decreased with a higher level of hypogravity unloading, the mean drop from 100 % to 80 % and 60 % effective body weight being about -9 ms (-2.7 %) and -23 ms (-6.5 %), respectively. In contrast, stance periods seemed to be virtually unaltered by hypogravity for the unloading levels studied. However, they decreased with higher running speeds as well, but to a lower extent as compared to step periods, the mean drop amounting to -1 ms (-0.8 %) per +1 km h^{-1} increase in running speed. Both findings are in qualitative accordance with recent results from other research groups (Barnes & Janecke, 2017; Thomson, Einarsson, Witvrouw, & Whiteley, 2017).

Second, concerning *spatial gait structure*, flight height became smaller with higher running speeds as a result of lower vertical take-off speeds, irrespective of the gravity level. Interestingly, the linear fits of vertical take-off speed as a function of running speed converge approximately at a common speed for all gravity levels studied, roughly corresponding to the running speed where vertical take-off speeds approach zero, i.e. at 57±4, 64±2 and 63±1 km h^{-1}. Notably, that "upper empirical limit" of running speed is far too high to be physiologically achievable by human running, the world record for 100 m corresponding to a speed of "only" about 38 km h^{-1}. Nonetheless, that convergence might reflect a common biomechanical adaptation that is present in all three gravity levels. Similarly, the common negative linear relation of flight height vs. step length across all gravity conditions and running speeds, as described by Eq. (13), might possibly reflect another commonality within the implicit (and rather subconscious) energetic optimization in human running motor control. The extrapolated hypothetical maximal step length of this trend (i.e. at zero flight height) amounts to 156±21 cm.

Moreover, vertical take-off speed *reduced* with lower gravity levels, i.e. higher hypogravity unloading, for a given running speed, thereby rendering steps *flatter* in hypogravity. This – at first sight paradoxical – finding is in agreement with recent results (Polet et al., 2017, 2018) and confirms that human motor control adapts to hypogravity in a counterintuitive manner by, among other factors, adjusting vertical take-off speed to lower values, and thus flattening the leaps. As Polet et al. have shown, energetic running efficiency is optimized by that biomechanical adaptation (Polet et al., 2017, 2018). Interestingly, the mean ratios of vertical take-off speed for 80 % vs. 100 % and 60 % vs. 100 % are 84±1 % and 68±1 %, respectively, and thus roughly match the gravity levels.

Third, *energy costs per step* were found to increase with higher running speed, irrespective of the gravity level, and significantly decreased with higher hypogravity unloading. This was physiologically expected and is in accordance with recent studies (Barnes & Janecke, 2017; R. Beneke & Leithäuser, 2017). Interestingly, energy costs per step amounted to 79±2 % and 66±2 % for 80 % vs. 100 % and 60 % vs. 100 % respectively, thereby approximately matching gravity levels. In other words, the energy costs per step in hypogravity approximately reduced proportionally to the gravity level γ, confirming that work against gravity possesses a predominant contribution to energy cost of running for a given running speed. In accordance to that, also the ratio of vertical vs. swing phase cost per step reduced approximately by the same amount as gravity was diminished, resulting in mean ratios of 90±4 % and 71±3 % for $\gamma = 80$ % and 60 % vs. 100 %, respectively.

Fourth, *energy costs per meter* were analogously attenuated by hypogravity approximately to the level of unloading, i.e. to 75±3 % and 58±3 % at $\gamma = 80$ % and 60 %, respectively. The finding that energy costs per meter were not constant with respect to running speed for a given gravity level, but increased with the onset of anaerobic (lactic) energy metabolism, provides a link to recent research results (R. Beneke & Leithäuser, 2017; Lacour & Bourdin, 2015; Minetti et al., 2002). In essence, there is now consensus that with anaerobic contributions, energy costs per meter increase (Lacour & Bourdin, 2015). Therefore, it is essential to measure not only respiratory parameters for aerobic, but also lactate accumulation for anaerobic contributions, when assessing energy expenditure at submaximal and maximal running speeds.

Fifth, the enhanced biomechanical model derived in this paper on the basis of the work of Polet and co-workers, showed a high degree of accordance to the experimental data. The refinement comprised two fitting operations: On the one hand, a linear, gravity-dependent relation between vertical take-off speed $v_{\perp}$ and running speed v_{run} was found in the experimentally obtained gait structure, which was used for modelling. On the other hand, the swing phase cost parameter A

, i.e. the gross equivalent to $A^{(\mathrm{net})}$ from Eq. (1), proved gravity and running speed dependent. A square root function best fitted the experimental data. Once the functional relations between $v_{\perp} = v_{\perp}(\gamma, v_{\mathrm{run}})$ and $A = A(\gamma, v_{\mathrm{run}})$ were set, energy costs and their relations were predicted with high accuracy. Therefore, the applicability and validity of Polet's model was verified in gross terms for competitive distance runners and triathletes in relevant running speeds of 12–22 km h^{-1} on a LBPPT. Future research on the yet unknown swing cost efficiency η_{swing} is proposed, linking gross and net values of swing cost via Eq. (15). Nonetheless, energy expenditure of a LBPPT exercise session can already be estimated for trained (male) athletes based on the results of this study. These outcomes might contribute, on the one hand, to improving training control, and, on the other hand, to defining LBPPT-specific training goals with focus on either aerobic or anaerobic training stimuli. By that, hypogravity treadmills might be employed in a more specific and effective way for various training purposes in the future.

Conclusion

In summary, it was experimentally shown that Eq. (1) provides a valid model for running on a LBPPT with gravity levels of $\gamma \geq 60\,\%$ and at running speeds of $12\ \mathrm{km\,h^{-1}} \leq v_{\mathrm{run}} \leq 22\ \mathrm{km\,h^{-1}}$, as being relevant to competitive distance running and triathlon. The gross swing cost parameter A proved gravity- and speed-dependent. Irrespective of gravity level, energy costs per meter were not constant with respect to running speed. Instead, with the onset of anaerobic lactic metabolism, they significantly increased. The experimental data on temporal and spatial gait structures revealed common trends for all gravity levels and running speeds studied, which may reflect converging biomechanical adaptations. The extrapolation of those common trends, e.g. flight height as a function of running speed, might possibly point at maximal theoretical values. In essence, the formalism proposed by Polet and refined in this study might help to further elucidate biomechanics of LBPPT running and its implications for exercise practice, and to design individually optimized training programs in artificial hypogravity.

List of symbols

A, $A^{(\mathrm{net})}$	Gross and net swing phase cot parameter
A_{ath}	Cross-sectional area of the athlete at the LBPPT girdle
$\vec{\boldsymbol{a}} \equiv \left(a_x, a_y, a_z\right)^{\mathrm{T}}$	3D acceleration vector and its three components
m	Mass of runner
$\vec{\boldsymbol{e}}_z$	Unit vector in z direction
f	Step frequency
$\vec{\boldsymbol{F}}_{\mathrm{G,\,eff}}$, $\vec{\boldsymbol{F}}_{\mathrm{G}}$, $\vec{\boldsymbol{F}}_{\Delta p}$	Effective and standard gravitational force, pressure gradient force
$g_0 \equiv 9.80665\ \mathrm{m\,s^{-2}}$	Constant of gravitational acceleration
$g \equiv \gamma g_0$	Effective gravitational acceleration
h_{flight}	Flight height of COM
p	Significance level
p_{i}, p_0	Internal and external pressure of LBPPT
$RQ \equiv \dot{V}_{\mathrm{CO_2}} \big/ \dot{V}_{\mathrm{O_2}}$	Respiratory quotient
$\overline{R}^2$	Adjusted coefficient of determination
s_{step}	Step length
T_{stride}, T_{step}, T_{stance}, $T_{\mathrm{step}}^{(0)}$, $T_{\mathrm{stance}}^{(0)}$	Stride, step, stance periods; …$^{(0)}$: linear fit intercepts
$v_{\perp}$	Vertical take-off speed
v_0	Linear fit intercept
v_{run}	Running speed
$\dot{V}_{\mathrm{O_2}}$, $\dot{V}'_{\mathrm{O_2}}$	Absolute and mass-related oxygen consumption
$W_{\dots}$, $W'_{\dots}$, $W''_{\dots}$, $W^{(\mathrm{net})}_{\dots}$	Gross energy expenditure (work), energy cost per step, energy cost per meter, net energy expenditure
W_{tot}, $W_{\dot{V}_{\mathrm{O_2}}}$, W_{La}, W_{CP}	Energy contributions: total, aerobic, lactic and alactic anaerobic
$W_{\perp}$, W_{swing}	Vertical and sing phase work / energy cost
α, β, δ_{step}, δ_{stance}	Linear fit coefficients
$\gamma \equiv BW_{\mathrm{Set}}$	Gravity level (percentage of standard gravity weight)
Δc_{La}	Change in blood lactate
Δp	Pressure difference
η, η_{swing}, η_{con}, η_{ecc}	Efficiency (total, swing phase, concentric and eccentric work)
$\eta_{\mathrm{partial}}^{\ 2}$	Partial portion of variance explained in an ANOVA, effect size
ζ	Square root scaling factor of A

References

Barnes, K. R., & Janecke, J. N. (2017). Physiological and Biomechanical Responses of Highly Trained Distance Runners to Lower-Body Positive Pressure Treadmill Running. *Sports Med Open, 3*(1), 41. doi:10.1186/s40798-017-0108-x

Barnes, K. R., & Kilding, A. E. (2015). Running economy: measurement, norms, and determining factors. *Sports Med Open, 1*(1), 8. doi:10.1186/s40798-015-0007-y

Beneke, R., Beyer, T., Jachner, C., Erasmus, J., & Hütler, M. (2004). Energetics of karate kumite. *European Journal of Applied Physiology, 92*(4), 518-523. doi:10.1007/s00421-004-1073-x

Beneke, R., & Hütler, M. (2005). The effect of training on running economy and performance in recreational athletes. *Med Sci Sports Exerc, 37*(10), 1794-1799. doi:10.1249/01.mss.0000176399.67121.02

Beneke, R., & Leithäuser, R. M. (2017). Energy Cost of Running Related to Running Intensity and Peak Oxygen Uptake. *Deutsche Zeitschrift für Sportmedizin, 68*(9), 196-202.

Bentley, D. J., Newell, J., & Bishop, D. (2007). Incremental exercise test design and analysis: implications for performance diagnostics in endurance athletes. *Sports Med, 37*(7), 575-586. doi:10.2165/00007256-200737070-00002

Borg, G. (1970). Perceived exertion as an indicator of somatic stress. *Scand J Rehabil Med, 2*(2), 92-98.

Cohen, J. (1973). Eta-Squared and Partial Eta-Squared in Fixed Factor Anova Designs. *Educational and Psychological Measurement, 33*(1), 107-112. doi:10.1177/001316447303300111

di Prampero, P. E. (1981). Energetics of muscular exercise. *Rev Physiol Biochem Pharmacol, 89*, 143-222.

Donelan, J. M., & Kram, R. (2000). Exploring dynamic similarity in human running using simulated reduced gravity. *J Exp Biol, 203*(Pt 16), 2405-2415.

Farina, K. A., Wright, A. A., Ford, K. R., Wirfel, L. A., & Smoliga, J. M. (2017). Physiological and Biomechanical Responses to Running on Lower Body Positive Pressure Treadmills in Healthy Populations. *Sports Med, 47*(2), 261-275. doi:10.1007/s40279-016-0581-2

Fleckenstein, D., Ueberschär, O., Wüstenfeld, J. C., & Wolfarth, B. (2018). Physiological and metabolic responses to lower body positive pressure treadmill running. *German Journal of Sports Medicine, 70*(9).

Hamacher, D., Hamacher, D., Taylor, W. R., Singh, N. B., & Schega, L. (2014). Towards clinical application: repetitive sensor position re-calibration for improved reliability of gait parameters. *Gait & posture, 39*(4), 1146-1148. doi:10.1016/j.gaitpost.2014.01.020

Hollander, K., Riebe, D., Campe, S., Braumann, K.-M., & Zech, A. (2014). Effects of footwear on treadmill running biomechanics in preadolescent children. *Gait & posture, 40*(3), 381-385. doi:10.1016/j.gaitpost.2014.05.006

Karatsidis, A., Bellusci, G., Schepers, H. M., de Zee, M., Andersen, M. S., & Veltink, P. H. (2016). Estimation of Ground Reaction Forces and Moments During Gait Using Only Inertial Motion Capture. *Sensors (Basel), 17*(1). doi:10.3390/s17010075

Karatsidis, A., Richards, R. E., Konrath, J. M., van den Noort, J. C., Schepers, H. M., Bellusci, G., . . . Veltink, P. H. (2018). Validation of wearable visual feedback for retraining foot progression angle using inertial sensors and an augmented reality headset. *Journal of NeuroEngineering and Rehabilitation, 15*(1), 78. doi:10.1186/s12984-018-0419-2

Kline, J. R., Raab, S., Coast, J. R., Bounds, R. G., McNeill, D. K., & de Heer, H. D. (2015). Conversion table for running on lower body positive pressure treadmills. *J Strength Cond Res, 29*(3), 854-862. doi:10.1519/jsc.0000000000000658

Lacour, J. R., & Bourdin, M. (2015). Factors affecting the energy cost of level running at submaximal speed. *Eur J Appl Physiol, 115*(4), 651-673. doi:10.1007/s00421-015-3115-y

Lusk, G. (1924). ANIMAL CALORIMETRY: Twenty-Fourth Paper. ANALYSIS OF THE OXIDATION OF MIXTURES OF CARBOHYDRATE AND FAT. *Journal of Biological Chemistry, 59*(1), 41-42.

Margaria, R. (1968). Positive and negative work performances and their efficiencies in human locomotion. *Internationale Zeitschrift für angewandte Physiologie einschließlich Arbeitsphysiologie, 25*(4), 339-351. doi:10.1007/BF00699624

McNeill, D. K., de Heer, H. D., Williams, C. P., & Coast, J. R. (2015). Metabolic accommodation to running on a body weight-supported treadmill. *Eur J Appl Physiol, 115*(5), 905-910. doi:10.1007/s00421-014-3071-y

McNeill, D. K., Kline, J. R., de Heer, H. D., & Coast, J. R. (2015). Oxygen consumption of elite distance runners on an anti-gravity treadmill(R). *J Sports Sci Med, 14*(2), 333-339.

Mercer, J. A., & Chona, C. (2015). Stride length–velocity relationship during running with body weight support. *Journal of Sport and Health Science, 4*(4), 391-395. doi:10.1016/j.jshs.2015.01.003

Minetti, A. E., Moia, C., Roi, G. S., Susta, D., & Ferretti, G. (2002). Energy cost of walking and running at extreme uphill and downhill slopes. *J Appl Physiol (1985), 93*(3), 1039-1046. doi:10.1152/japplphysiol.01177.2001

Moran, M. F., Rickert, B. J., & Greer, B. K. (2017). Tibial Acceleration and Spatiotemporal Mechanics in Distance Runners During Reduced-Body-Weight Conditions. *J Sport Rehabil, 26*(3), 221-226. doi:10.1123/jsr.2015-0141

Munoz Diaz, E., Kaiser, S., & Bousdar Ahmed, D. (2018). Height Error Correction for Shoe-Mounted Inertial Sensors Exploiting Foot Dynamics. *Sensors (Basel), 18*(3). doi:10.3390/s18030888

Polet, D. T., Schroeder, R. T., & Bertram, J. E. A. (2017). Reducing gravity takes the bounce out of running. *The Journal of Experimental Biology, 221*. doi:10.1242/jeb.162024

Polet, D. T., Schroeder, R. T., & Bertram, J. E. A. (2018). Correction: Reducing gravity takes the bounce out of running (doi:10.1242/jeb.162024). *The Journal of Experimental Biology, 221*(17).

Richardson, J. T. E. (2011). Eta squared and partial eta squared as measures of effect size in educational research. *Educational Research Review, 6*(2), 135-147. doi:https://doi.org/10.1016/j.edurev.2010.12.001

Shaw, A. J., Ingham, S. A., & Folland, J. P. (2014). The valid measurement of running economy in runners. *Med Sci Sports Exerc, 46*(10), 1968-1973. doi:10.1249/mss.0000000000000311

Squadrone, R., & Gallozzi, C. (2009). Biomechanical and physiological comparison of barefoot and two shod conditions in experienced barefoot runners. *J Sports Med Phys Fitness, 49*(1), 6-13.

Strohrmann, C., Harms, H., Kappeler-Setz, C., & Troster, G. (2012). Monitoring kinematic changes with fatigue in running using body-worn sensors. *IEEE Trans Inf Technol Biomed, 16*(5), 983-990. doi:10.1109/titb.2012.2201950

Thomson, A., Einarsson, E., Witvrouw, E., & Whiteley, R. (2017). Running speed increases plantar load more than per cent body weight on an AlterG® treadmill. *J Sports Sci, 35*(3), 277-282. doi:10.1080/02640414.2016.1163401

Ueberschär, O., Fleckenstein, D., Warschun, F., Kränzer, S., Walter, N., & Hoppe, M. W. (2019). Measuring biomechanical loads and asymmetries in junior elite long-distance runners through triaxial inertial sensors. *Sports Orthopeadics and Traumatology, 35*(3). doi:10.1016/j.orthtr.2019.06.001

Ueberschär, O., Fleckenstein, D., Warschun, F., Walter, N., & Hoppe, M. W. (2019). Case report on lateral asymmetries in two junior elite long-distance runners during a high-altitude training camp *Sports Orthopaedics and Traumatology, 35*(3). doi:10.1016/j.orthtr.2019.06.002

Ueberschär, O., Fleckenstein, D., Wüstenfeld, J. C., Warschun, F., Falz, R., & Wolfarth, B. (2019). Running on the hypogravity treadmill AlterG® does not reduce the magnitude of peak tibial impact accelerations. *Sports Orthopaedics and Traumatology, 35*(3).

Zagatto, A. M., Leite, J. V., Papoti, M., & Beneke, R. (2016). Energetics of Table Tennis and Table Tennis-Specific Exercise Testing. *Int J Sports Physiol Perform, 11*(8), 1012-1017. doi:10.1123/ijspp.2015-0746